

# A Stability Analysis of Wavelet based Numerical methods of Dynamic Reynolds Equation for Micro-polar Fluid Lubrication

S.N. Gaikwad<sup>1</sup>, Sanjivappa K Dembare<sup>2</sup>

<sup>1</sup>Professor, Department of Mathematics, Gulbarga University, Jnana Ganga Campus, Gulbarga 585 106, India, Email: sngaikwad2009@yahoo.co.in

<sup>2</sup>Research Scholar, Department of Mathematics, Gulbarga University, Jnana Ganga Campus, Gulbarga 585 106, India, Email: skdembare@gmail.com

---

Received: 11.04.2024

Revised : 16.05.2024

Accepted: 24.05.2024

---

## ABSTRACT

Recently, wavelet theory has emerged as a reliable and promising tool in the fields of engineering and research. Wavelets are effectively employed in swift algorithms for informal execution. This study offers a comprehensive stability analysis of a wavelet lifting method utilising both orthogonal and biorthogonal wavelets to address the dynamic stability issue. The application of the Reynolds equation to the lubrication of micropolar fluids is exceptionally innovative. Wavelet approaches are recognised for their ability to effectively address issues involving both spatial and temporal variations. Consequently, they are appropriate for addressing dynamic fluid equations, including the Reynolds equation.

**Keywords:** Stability analysis, Lifting scheme; Orthogonal and biorthogonal wavelets; Reynolds equation; Micro-polar fluid lubrication.

## 1. INTRODUCTION

Micropolar fluids indeed present a fascinating area of study within fluid dynamics, particularly due to their unique characteristics involving suspended particles with rotational inertia and microstructure effects. Here are some points that can further elaborate on the significance and applications of micropolar fluids [1, 2]:

- I. **Definition and Characteristics:** Micropolar fluids are characterized by the inclusion of microstructural effects such as local rotational inertia and couple stresses. Unlike classical Newtonian fluids, which assume a continuum without internal structure, micropolar fluids model the internal rotation and translation of small particles within the fluid.
- II. **Origin and Development:** The theory of micropolar fluids was introduced by Eringen as an extension of continuum mechanics to incorporate microstructural effects. This includes the inertia of rotational motion and the interaction between rotation and translation of fluid elements, which are not accounted for in classical fluid dynamics.
- III. **Applications:** Micropolar fluid models find applications in a wide range of fields, including:
  - **Lubricants:** Studying the behavior of micropolar lubricants is crucial for understanding friction and wear mechanisms at small scales, relevant for improving efficiency in machinery.
  - **Suspensions and Colloids:** Understanding the flow properties of suspensions and colloidal fluids, where particles exhibit complex interactions and contribute significantly to the overall rheology.
  - **Biological Fluids:** Modeling blood flow, where the suspension of red blood cells affects viscosity and flow patterns, is another critical application.
  - **Polymer Dynamics:** Micropolar fluid theory aids in understanding the flow behavior of polymer melts and solutions, where polymer chains can exhibit rotational and translational degrees of freedom.
- IV. **Advantages in Non-Newtonian Flow:** Micropolar fluid models are particularly useful in describing non-Newtonian behavior, where shear-thinning or shear-thickening effects are observed due to the microstructural interactions. This makes micropolar fluids applicable to a broader range of industrial and biological fluids compared to classical fluid models.
- V. **Numerical and Theoretical Challenges:** Solving equations for micropolar fluids often involves complex mathematical formulations, requiring advanced numerical techniques like the wavelet lifting scheme you mentioned. These methods are crucial for accurately capturing the microscale effects while maintaining computational efficiency.

Micropolar fluid theory has gained significant attention in research due to its applicability across various industrial processes and phenomena that classical Navier-Stokes theory struggles to adequately describe. Micropolar fluid theory has been employed by researchers to examine various bearing systems, including slider bearings. Slider bearings are mechanical devices that facilitate and direct the motion of machine components, such as shafts or rods, by minimising friction and wear via fluid lubrication. Journal bearings, squeeze film bearings, and porous bearings have demonstrated certain advantages of micropolar fluids over Newtonian lubricants, including enhanced load-carrying capacity and prolonged time of approach for squeeze film bearings. Naduvinamani and Marali [7], Naduvinamani et al. [8], and Naduvinamani and Santosh [9] investigated the effects on modified Reynolds equations for micropolar fluid lubrication utilising the finite difference method [FDM]. This work proposes a stability analysis of the wavelet lifting scheme for solving the modified Reynolds equation in micropolar fluid lubrication.

Wavelet analysis has fundamentally transformed signal and image processing since its emergence in the 1980s. This is a comprehensive examination of its importance, evolution, and uses by Stromberg [10], Grossmann and Morlet [11], and Meyer [12]. The multiresolution approximation by Mallat and Meyer resulted in the orthogonal wavelet family developed by Daubechies. Wavelets have found widespread applications in numerous engineering fields, chiefly owing to their efficacy in signal analysis, time-frequency analysis, and numerical approaches for resolving systems of equations. Early research on wavelet-based approaches is documented in Dahmen et al. [16]. A compilation of the discrete wavelet transforms (DWT) and the recently announced wavelet-based multigrid technique as referenced in [17-19]. Shiralashetti and Kantli [20, 21] proposed a modified wavelet multigrid approach for solving boundary value problems. The biorthogonal wavelet approach is also utilised for solving elliptic partial differential equations [22]. The integration of wavelet transforms and multigrid approaches provides an effective toolkit for efficiently addressing intricate computational challenges. It utilises the capacity of wavelets to depict signals at various resolutions and the iterative enhancement of multigrid techniques to attain precise solutions with diminished computing expense. The wavelet-based lifting approach was presented by Sweldens [24], enabling advancements in the properties of established wavelet transforms. The approach offers numerous numerical advantages, including a diminished number of operations, which are essential in the context of iterative solvers. Shiralashetti and Kantli [25, 26] offer a wavelet-based lifting technique as an innovative method to address complex issues in elasto-hydrodynamic lubrication and nonlinear partial differential equations. Its implementation in practical situations illustrates its potential advantages regarding precision, computational efficiency, and relevance to intricate engineering and scientific challenges. This demonstrates the method's potential to substantially enhance computational techniques in these domains.

The rest of the article is ordered as follows: Preliminaries of wavelets are given in section 2. Section 3 devotes the mathematical formulation of problem. Numerical stability of the problem is presented in section 4. Section 5 results and discussion. Finally, concluding remarks of the paper are discussed in section 6.

## 2. Preliminaries of wavelets

The orthogonality and smoothness conditions required for scaling and wavelet functions form the basis for the simultaneous construction of orthogonal and biorthogonal wavelet coefficients. The value of the filter coefficients is constrained by dilation equations due to these circumstances. We possess two distinct functions that delineate the refinement relation. These functions are referred to as scaling functions and

wavelet functions, both of which encompass coefficients  $\{h_{jm}\}$  and  $\{g_{jm}\}$ . The coefficients dictate the form of the scaling and wavelet functions, which furthermore function as signal filters. The coefficients dictate the application in which the specific wavelet can be utilised. Although a substantial amount of information exists regarding filter design for certain applications, it remains inaccessible to the typical reader. This is because nearly all methods utilise frequency domain and complex analytical concepts to develop the filter.

### 2.1. Wavelet filters

The primary categories of filters are finite impulse response (FIR) filters. The primary attributes of these filters are their advantageous time-localization properties. These filters are derived from wavelets with compact support and are designed such that,

$$h_{jm} = 0 \quad \text{for } n < 0 \quad \text{and } n > L_1$$

in which  $L_1$  is the length of the filter.

The minimum requirements for these compact FIR filters are:

a) The length of the scaling filter  $h_{fn}$  must be even.

$$b) \sum_n h_{fn} = \sqrt{2}$$

$$c) \sum_n (h_{fn} \cdot h_{fn-2m}) = \delta(m),$$

in which  $\delta(m)$  is the Kronecker delta, such that, it is equal to 1 for  $m = 0$  or 0 for  $m = 1$ .

## 2.2. Haar wavelet filter coefficients

We know that low pass filter coefficients  $h_f = [h_{f0}, h_{f1}]^T = \left[ \frac{\sqrt{2}}{2}, \frac{\sqrt{2}}{2} \right]^T$  and high pass filter

coefficients  $g_f = [g_{f0}, g_{f1}]^T = \left[ \frac{\sqrt{2}}{2}, \frac{\sqrt{2}}{2} \right]^T$  play an important role in the decomposition.

## 2.3. Daubechies wavelet filter coefficients

Daubechies introduced scaling functions that satisfy the above requirements and distinguished by having the shortest possible support. The scaling function  $\phi$  has support  $[0, L_1 - 1]$ , while the corresponding wavelet  $\Psi$  has support in the interval  $[1 - L_1 / 2, L_1 / 2]$ . We have filter coefficients [27],

$$h_f = [h_{f0}, h_{f1}, h_{f2}, h_{f3}]^T = \left[ \frac{1+\sqrt{3}}{4\sqrt{2}}, \frac{3+\sqrt{3}}{4\sqrt{2}}, \frac{3-\sqrt{3}}{4\sqrt{2}}, \frac{1-\sqrt{3}}{4\sqrt{2}} \right]^T$$
 are low pass filter coefficients

and  $g_f = [g_{f0}, g_{f1}, g_{f2}, g_{f3}]^T = \left[ \frac{1-\sqrt{3}}{4\sqrt{2}}, -\frac{3-\sqrt{3}}{4\sqrt{2}}, \frac{3+\sqrt{3}}{4\sqrt{2}}, -\frac{1+\sqrt{3}}{4\sqrt{2}} \right]^T$  are the high pass filter coefficients.

## 2.4. Biorthogonal (CDF (2, 2)) wavelet filter coefficients

In numerous filtering applications, symmetrical filter coefficients are required to achieve enhanced accuracy. All orthogonal wavelet systems, with the exception of Haar, lack symmetrical coefficients. However, Haar is inadequate for numerous applications in science and engineering. A biorthogonal wavelet system can be designed to possess this characteristic. This serves as the impetus for the design of such wavelet systems. The subsequent biorthogonal (CDF (2, 2)) wavelet filter coefficients are as follows: [28, 29],

$$\text{Low pass filters: } h_f = [h_{f0}, h_{f1}, h_{f2}] = \left[ \frac{1}{2\sqrt{2}}, \frac{1}{\sqrt{2}}, \frac{1}{2\sqrt{2}} \right] \text{ and}$$

$$\tilde{h}_f = [\tilde{h}_{f0}, \tilde{h}_{f1}, \tilde{h}_{f2}, \tilde{h}_{f3}, \tilde{h}_{f4}] = \left[ \frac{-\sqrt{2}}{8}, \frac{\sqrt{2}}{4}, \frac{3\sqrt{2}}{4}, \frac{\sqrt{2}}{4}, \frac{-\sqrt{2}}{8} \right].$$

Similarly, high pass filters:  $g_{fm} = (-1)^m \tilde{h}_{f4-m}$  and  $\tilde{g}_{fm} = (-1)^{m+1} h_{f2-m}$ .

## 3. Mathematical formulation of the problem

The basic equations governing the flow of micropolar lubricants [1] under the usual assumptions of lubrication theory for thinfilms are [30]

$$\left( \mu + \frac{\chi}{2} \right) \frac{\partial^2 u}{\partial y^2} + \chi \frac{\partial v_3}{\partial y} - \frac{\partial p}{\partial x} = 0 \quad (3.1)$$

$$\frac{\partial p}{\partial y} = 0 \quad (3.2)$$

$$\left(\mu + \frac{\chi}{2}\right) \frac{\partial^2 w}{\partial y^2} + \chi \frac{\partial v_1}{\partial y} - \frac{\partial p}{\partial z} = 0 \quad (3.3)$$

$$\gamma \frac{\partial^2 v_1}{\partial y^2} - 2\chi v_1 + \chi \frac{\partial w}{\partial y} = 0 \quad (3.4)$$

$$\gamma \frac{\partial^2 v_3}{\partial y^2} - 2\chi v_3 - \chi \frac{\partial u}{\partial y} = 0 \quad (3.5)$$

$$\frac{\partial u}{\partial x} + \frac{\partial v}{\partial y} + \frac{\partial w}{\partial z} = 0 \quad (3.6)$$

where  $u$ ,  $v$  and  $w$  are the velocity components of the lubricant in the  $x$ ,  $y$  and  $z$  direction, respectively and  $(v_1, v_2, v_3)$  are micro rotational velocity components. And also  $\chi$  is the spin viscosity,  $\gamma$  is the viscosity coefficient for micropolar fluids,  $p$  is the pressure and  $\mu$  is the Newtonian viscosity coefficient.

The flow of micropolar lubricants in a porous matrix governed by the modified Darcy law, which account for the polar effects is given by

$$q^* = \frac{-k}{(\mu + \chi)} \nabla p^* \quad (3.7)$$

where  $q^* = (u^*, v^*, w^*)$  is the modified Darcy velocity vector,  $k$  is the permeability of the porous matrix,  $p^*$  is the pressure in the porous matrix and  $u^*$ ,  $v^*$ ,  $w^*$  are the modified Darcy's velocity components in the  $x$ ,  $y$ ,  $z$  directions, respectively, they are

$$u^* = \frac{-k}{(\mu + \chi)} \frac{\partial p^*}{\partial x}, \quad v^* = \frac{-k}{(\mu + \chi)} \frac{\partial p^*}{\partial y}, \quad w^* = \frac{-k}{(\mu + \chi)} \frac{\partial p^*}{\partial z}.$$

Due to continuity of the fluid in the porous matrix, the pressure  $p^*$  satisfies the Laplace equation

$$\frac{\partial^2 p^*}{\partial x^2} + \frac{\partial^2 p^*}{\partial y^2} + \frac{\partial^2 p^*}{\partial z^2} = 0. \quad (3.8)$$

The relevant boundary conditions for the velocity components are

(i) At the bearing surface ( $y = 0$ )

$$u = w = 0, \quad v = v^* \quad (3.9a)$$

$$v_1 = v_3 = 0 \quad (3.9b)$$

(ii) At the journal surface ( $y = h$ )

$$u = w = 0, \quad v = \frac{\partial h}{\partial t} \quad (3.10a)$$

$$v_1 = v_3 = 0 \quad (3.10b)$$

The generalized Reynolds type equation is given by Naduvanamani et al. [8]

$$\frac{\partial}{\partial x} \left[ \left( f(h, l, \beta) + \frac{12\mu k H}{(\mu + \chi)} \right) \frac{\partial p}{\partial x} \right] + \frac{\partial}{\partial z} \left[ \left( f(h, l, \beta) + \frac{12\mu k H}{(\mu + \chi)} \right) \frac{\partial p}{\partial z} \right] = 12\mu \frac{\partial h}{\partial t} + 6\mu U \frac{\partial h}{\partial x} \quad (3.11)$$

where

$$f(h, l, \beta) = h^3 + 12l^2 h - 6\beta l h^2 \coth\left(\frac{\beta h}{2l}\right) \quad (3.12)$$

$$\text{and } h = a \left( 1 - \frac{x}{L} \right)$$

where  $U$  is the sliding velocity,  $H$  is the porous layer thickness,  $\beta = \left(\frac{\chi}{\chi + 2\mu}\right)^{1/2}$  is the coupling number,  $h$  is the film thickness function and  $l = \left(\frac{\gamma}{4\mu}\right)^{1/2}$  is the characteristic length.

Introducing the following non-dimensional quantities;

$$h_1 = \frac{h}{h_{m0}}, P = \frac{ph_{m0}^2}{LU\mu}, t_1 = \frac{Ut}{L}, x_1 = \frac{x}{L}, z_1 = \frac{z}{B}, \psi = \frac{kH}{h_{m0}^3}, l_1 = \frac{l}{h_{m0}}$$

where  $L$  is length of the bearing,  $t$  is the time and  $B$  is the width of the bearing.

After using the above quantities, the above modified Reynolds equation can be expressed in a non-dimensional form as

$$\frac{\partial}{\partial x_1} \left[ \left\{ f_1(h_1, l_1, \beta) + 12\psi \left( \frac{1-\beta^2}{1+\beta^2} \right) \right\} \frac{\partial P}{\partial x_1} \right] + \frac{1}{\delta^2} \frac{\partial}{\partial z_1} \left[ \left\{ f_1(h_1, l_1, \beta) + 12\psi \left( \frac{1-\beta^2}{1+\beta^2} \right) \right\} \frac{\partial P}{\partial z_1} \right] = -6\lambda \quad (3.13)$$

where

$$f_1(h_1, l_1, \beta) = h_1^3 + 12l_1^2 h_1 - 6\beta l_1 h_1^2 \coth \left( \frac{\beta h_1}{2l_1} \right) \quad (3.14)$$

and  $h_1 = \alpha(1-x_1)$ , where  $\alpha = \left(\frac{a}{h_{m0}}\right)$  is the slider-profile parameter,  $a$  is the difference between the

inlet and outlet film thickness and  $\delta = \frac{B}{L}$  is aspect ratio of the bearing. The steady and dynamic characteristics of the porous bearings are obtained by using the perturbations in steady-state minimum film thickness at the outlet  $h_{m0}$ .

The boundary conditions for the fluid film pressure are

$$P = 0 \text{ at } x_1 = 0, x_1 = 1, z_1 = 0, z_1 = 1 \quad (3.15)$$

The modified Reynolds equation is solved numerically by using FDM. In finite increment format, the Eq. (4.13) can be expressed as

$$P_{i,j} = c_1 P_{i+1,j} + c_2 P_{i-1,j} + c_3 P_{i,j+1} + c_4 P_{i,j-1} + c_5 \quad (3.16)$$

The coefficients  $c_0$  to  $c_5$  are defined as

$$c_1 = \delta^2 b^2 \left( f_{1i+\frac{1}{2},j} + 12\psi \left( \frac{1-\beta^2}{1+\beta^2} \right) \right) / c_0 \quad (3.17)$$

$$c_2 = \delta^2 b^2 \left( f_{1i-\frac{1}{2},j} + 12\psi \left( \frac{1-\beta^2}{1+\beta^2} \right) \right) / c_0 \quad (3.18)$$

$$c_3 = c_4 = \left( f_{1i,j} + 12\psi \left( \frac{1-\beta^2}{1+\beta^2} \right) \right) / c_0 \quad (3.19)$$

$$c_5 = 6\delta^2 \lambda (\Delta z_1)^2 / c_0 \quad (3.20)$$

where

$$c_0 = \delta^2 b^2 \left( f_{1i+\frac{1}{2},j} + 12\psi \left( \frac{1-\beta^2}{1+\beta^2} \right) + f_{1i-\frac{1}{2},j} + 12\psi \left( \frac{1-\beta^2}{1+\beta^2} \right) \right) + 2 \left( f_{1i,j} + 12\psi \left( \frac{1-\beta^2}{1+\beta^2} \right) \right) \quad (3.21)$$

and  $b = \Delta z_1 / \Delta x_1$ .

The fluid film pressure  $P$  is calculated by using FDM.

The load carrying capacity  $W$  is obtained by integrating the fluid film pressure over the film region.

$$W = \frac{\mu UL^2 B}{h_{m0}^2} \int_{x=0}^{x=L} \int_{z=0}^{z=B} p dx dz, \tag{3.22}$$

which is in non-dimensional form

$$W_1 = \frac{Wh_{m0}^2}{\mu UL^2 B} = \int_{x_1=0}^{x_1=1} \int_{z_1=0}^{z_1=1} P dx_1 dz_1, \tag{3.23}$$

$$\approx \sum_{i=0}^M \sum_{j=0}^{M_1} P_{i,j} \Delta x_1 \Delta z_1$$

where  $M + 1$  and  $M_1 + 1$  are the grid-point numbers in the  $x_1$  and  $z_1$  directions respectively, having  $N = (M + 1) \times (M_1 + 1)$  equations with  $N$  unknowns to determine.

**4. Numerical Method and Stability of the problem**

By applying the FDM to Eq. (3.16), which gives the system of algebraic equations,  $Au = F$  (4.1)

where  $A$  is  $N \times N$  coefficient matrix,  $F$  is  $N \times 1$  matrix and  $u$  is  $N \times 1$  matrix to be determined.

By solving Equation (4.1), we derive an approximate solution. The needed answer is the sum of the approximate solution and the error, as the approximate solution contains some error. Numerous techniques exist to mitigate such errors and provide an accurate solution. Among them are multigrid, wavelet multigrid, modified wavelet multigrid, and biorthogonal wavelet multigrid approaches, among others. We are currently employing an advanced technique utilising orthogonal and biorthogonal wavelets known as the wavelet lifting scheme. Recently, lifting techniques have proven to be highly beneficial in signal analysis and image processing within the realms of science and engineering. However, it currently encompasses approximations in numerical analysis. This discussion pertains to the algorithm [23] of the wavelet lifting method as follows.

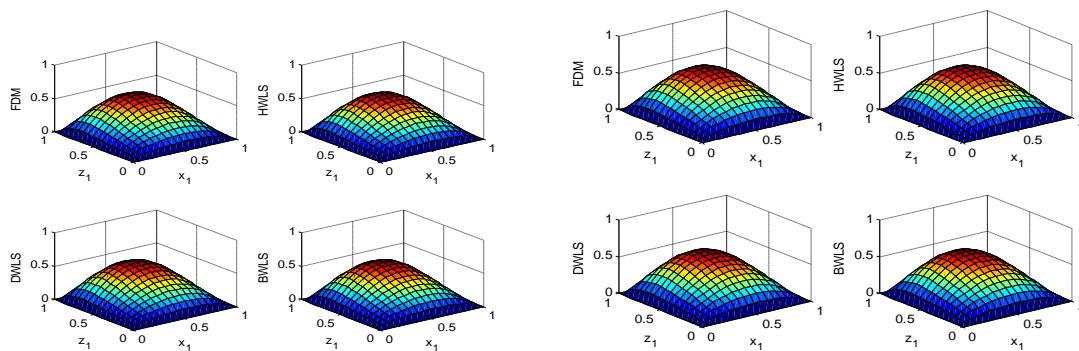
**4.1. Wavelet lifting schemes**

Daubechies and Sweldens [30] shown that any wavelet filter may be expressed as a series of lifting steps. Additional information regarding the benefits and other significant structural advantages of the lifting technique is available in [23, 24]. The novel methodologies are exemplified through various numerical problems, with the findings shown in the subsequent section.

**4.2. Numerical Stability**

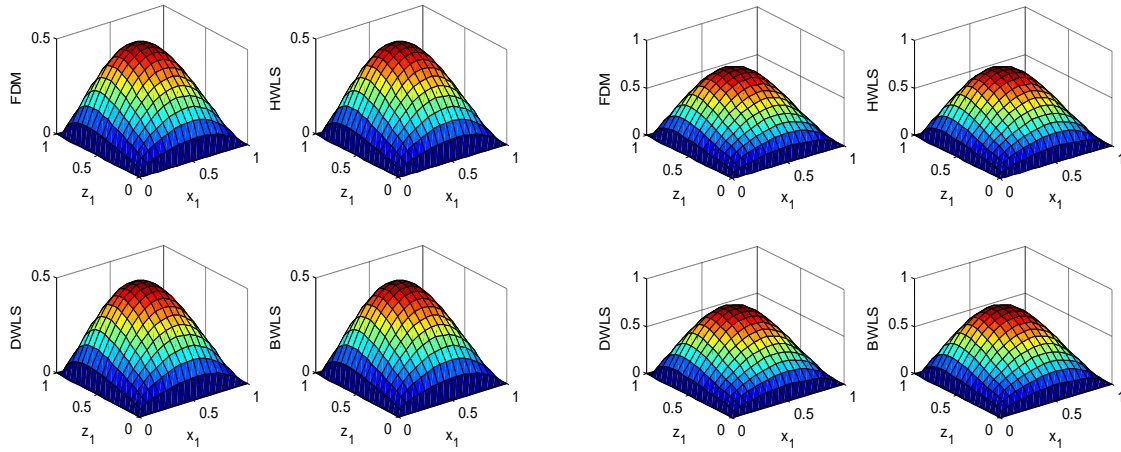
For the purpose of establishing the validity and applicability of these wavelet algorithms, the numerical stability of the Haar Wavelet Lifting Scheme (HWLS), the Daubechies Wavelet Lifting Scheme (DWLS), and the Biorthogonal Wavelet Lifting Scheme (BWLS) is demonstrated in this article.

Within the context of demonstrating the utility of the technique, we take into consideration the modified Reynolds equation. With the assistance of the equation (3.16), we are able to ascertain the pressure of the fluid layer, and the answers to this equation are presented in the figures that follow for a number of different factors.



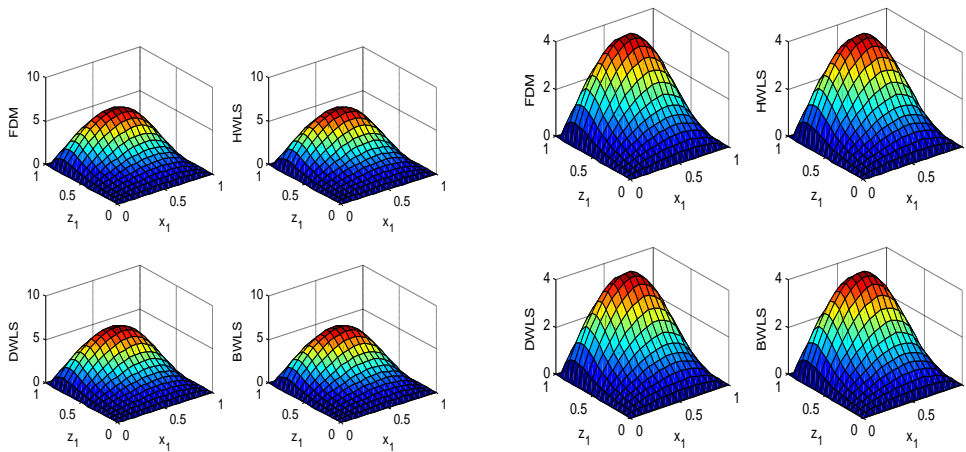
(a)  $l_1=0$  (Newtonian) (b)  $l_1=0.2$

**Figure 1.** Comparison of numerical solutions of fluid film pressure  $P$  of problem for  $N=256$  for  $\alpha = 1.6$ ,  $\delta = 2.5$ ,  $\psi = 0.25$  and  $\beta = 0.5$ .



(a)  $\beta = 0.25$  (b)  $\beta = 0.5$

Figure 2. Comparison of numerical solutions of fluidfilm pressure Pof test problem for N=256 for  $\alpha = 1.6$ ,  $\delta = 2.5$ ,  $l_1 = 0.15$  and  $\psi = 0.2$ .



(a)  $\psi = 0.05$  (b)  $\psi = 0.075$

Figure 3. Comparison of numerical solutions of fluidfilm pressure Pof test problem for N=256 for  $\alpha = 1.6$ ,  $\delta = 2.5$ ,  $l_1 = 0.2$  and  $\beta = 0.8$ .

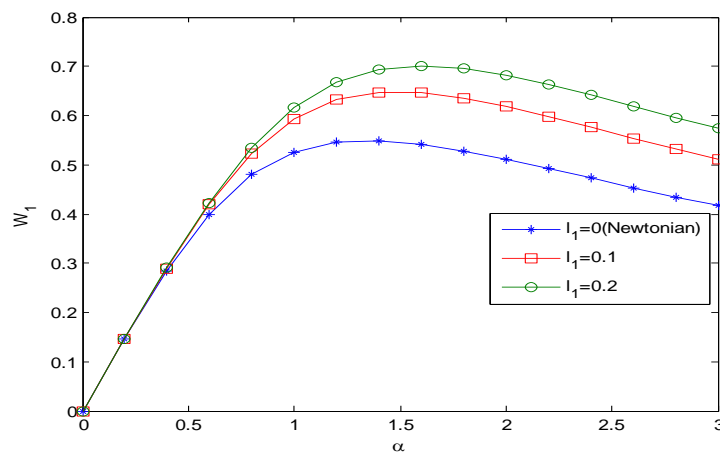
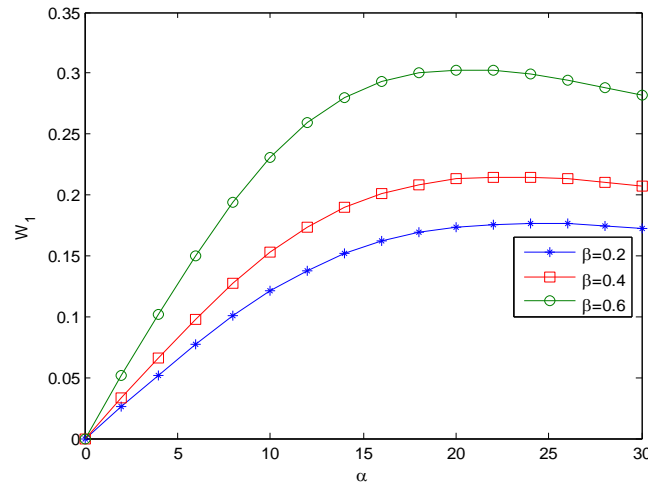
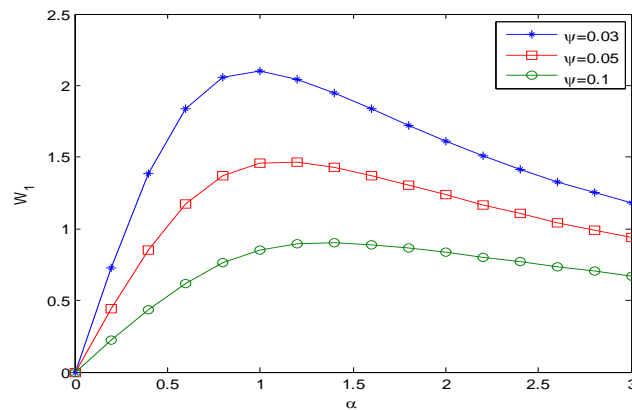


Figure 4. Variation of non-dimensional steady load-carrying capacity  $W_1$  with profile parameter  $\alpha$  for N=256 for  $\delta = 1.5$ ,  $\psi = 0.15$  and  $\beta = 0.8$ .



**Figure 5.** Variation of non-dimensional steady load-carrying capacity  $W_1$  with profile parameter  $\alpha$  for  $N=256$  for  $\delta = 1.5$ ,  $\psi = 0.2$  and  $l_1 = 0.15$ .



**Figure 6.** Variation of non-dimensional steady load-carrying capacity  $W_1$  with profile parameter  $\alpha$  for  $N=256$  for  $\delta = 1.5$ ,  $l_1 = 0.15$  and  $\beta = 0.8$ .

**Table 1.** The maximum residual with CPU time (in seconds) versus grid points of problem.

N	Method	$Re s_{max}$	Setup time	Running time	Total time
8X8	FDM	8.8080e-03	3.6203e+00	7.5332e-02	3.6956e+00
	HWLS	8.9070e-03	7.1466e-04	1.3209e-03	2.0355e-03
	DWLS	8.9070e-03	6.0348e-04	6.1302e-03	6.7337e-03
16X16	BWLS	8.9060e-03	5.0632e-04	1.3305e-03	1.8368e-03
	FDM	5.8205e-03	3.3504e+00	4.9923e-02	3.4003e+00
	HWLS	5.8105e-03	6.9447e-04	1.2805e-03	1.9750e-03
32X32	DWLS	5.8105e-03	5.9766e-04	6.0915e-03	6.6892e-03
	BWLS	5.8100e-03	4.8202e-04	2.6753e-03	3.1573e-03
	FDM	9.5308e-04	1.0617e+01	5.6666e-02	1.0674e+01
32X32	HWLS	9.5350e-04	6.7155e-04	1.2716e-03	1.9432e-03
	DWLS	9.5355e-04	5.8500e-04	6.0871e-03	6.6721e-03
	BWLS	9.5208e-04	4.8545e-04	2.7050e-03	3.1905e-03

**5. RESULTS AND DISCUSSION**

We were able to obtain the results of the challenge by using the MatLab software. It is essential to include the two non-dimensional elements while analysing the lubricating properties of micropolar fluids. To define the relationship between Newtonian viscosities and microrotational viscosities, the coupling number  $\beta$  denotes this interaction. If  $\chi$  quantity approaches 0, it consequently  $\beta$  approaches zero, as



per the definition. The characteristic length  $l_1$  is the second parameter, responsible for delineating the interaction between the micropolar fluid and the film gap. The permeability parameter  $\psi$  is utilised to analyse the influence of permeability on the static and dynamic qualities of bearings. It has been observed that  $l_1 \rightarrow 0$  the issue can be simplified to the corresponding Newtonian scenario. Figure 1 illustrates the variation in the non-dimensional fluid film pressure  $P$  for several distinct values of characteristic length  $l_1$ . Consequently,  $l_1$  an increase in values has led to a slight rise in  $P$ . The variation in non-dimensional fluid sheet pressure  $P$  is depicted in Figure 2, illustrating its dependence on different coupling number  $\beta$  values. Moreover, it has been found that the film pressure significantly escalates with an increase in the value of  $\beta$ . Figure 3 illustrates the fluctuation of the non-dimensional pressure  $P$  for various values of  $\psi$  the permeability parameter. The pressure  $P$  decreases as the values  $\psi$  in the equation grow.

Figure 4 illustrates the variance in dimensionless load-carrying capacity as a function of the profile parameter for several distinct values of the characteristic length. Moreover, it has been found that it expands as the values increase. An important element to examine is the critical value of 1.6, which is the point at which  $W1$  attains its maximum. Furthermore, it is crucial to emphasise that the influence of characteristic length  $l_1$  increases  $W1$  relative to the Newtonian scenario, where  $l_1$  is zero.

Figure 5 illustrates the variation of  $W1$  in relation to the profile parameter  $\alpha$  for various values of the coupling number. The observation that the critical value decreases as the value grows is noteworthy.

Figure 6 illustrates the variation of  $W1$  in relation to different values of the permeability parameter  $\psi$ . The value of  $W1$  grows as the value of  $\psi$  falls. Furthermore, it is essential to note that the critical value at which  $W1$  attains its maximum value is. An elevation in  $\psi$  leads to an augmentation in value  $\psi$ .

## CONCLUSIONS

This research aims to present an efficient wavelet lifting approach that incorporates both orthogonal and biorthogonal wavelets inside its framework. To illustrate the consistency of our methodology, we utilise this scheme to analyse the dynamic Reynolds equation that regulates micropolar fluid lubrication. The accuracy of our methodology is corroborated by numerical results presented in tables and figures, demonstrating the method's extensive applicability across many scientific and technical disciplines.

## REFERENCES

- [1] Eringen, A. C., Theory of micropolar fluids, *J. Math. Mech.* 16 (1), (1966) 1-18.
- [2] Eringen, A. C., Simple microfluids, *Int. J. Engg. Sci.* 2, (1964) 205-217.
- [3] Singh, C., Sihna, P., The three-dimensional Reynolds equation for micropolar fluid lubricated bearings, *Wear*, 76, (1982) 199-209.
- [4] Khonasari, M. M., Brewes, D. E., On the performance of finite journal bearings lubricated with micropolar fluids, *Trib. Trans.* 32 (2), (1989) 155-160.
- [5] Bujurke, N. M., Bhavi, S. G., Hiremath, P. S., Squeeze film lubricated with micropolar Fluids, *Proc. Ind. Nat. Sci. Acad.* 53 (3), (1987) 391-398.
- [6] Zaheeruddin, K. H., Isa, M., One-dimensional porous journal bearing lubrication with micropolar fluid, *Wear*, 83, (1980) 257-268.
- [7] Naduvinamani, N. B., Marali, G. B., Dynamic Reynolds equation for Micropolar fluid lubrication of Porous slider bearings, *J. Marine Sci. Tech.* 16 (3), (2008) 182-190.
- [8] Naduvinamani, N. B., Santosh, S., Siddanagouda, A., On the Squeeze film lubrication of rough short porous partial journal bearings with micropolar fluids, *J. Engg. Trib.* 224, (2009) 249-257.
- [9] Naduvinamani, N. B., Santosh, S., Micropolar Fluid Squeeze Film Lubrication of Finite Porous Journal Bearing, *Proc. 13<sup>th</sup> Asian Cong. Fluid Mech.* (2010) 970-973.
- [10] Stromberg, J. O., A modified Franklin system and higher order spline systems on  $R^n$  as unconditional bases for Hardy spaces, in: *Conference on Harmonic Analysis II*, adsworth International, CA, (1981) 466-494.
- [11] Grossmann, A., Morlet, J., Decomposition of Hardy functions into square integrable wavelet of constant shape, *SIAM J. Math. Anal.* 15, (1984) 723-736.
- [12] Meyer, Y., Wavelets and operators, in: E. Berkson, T. Peck, J. Uhl (Eds.), *Analysis at Urbana I: Analysis in Function Spaces*, Cambridge University Press, Cambridge, (1989) 256-365.
- [13] Mallat, S. G., Multiresolution approximations and wavelet orthonormal bases of  $L^2(R)$ , *Trans. Am. Math. Soc.* 315, (1989) 69-87.

- [14] Meyer, Y., Principe d'incertitude, bases Hilbertiennes et algebres d'operateurs, Seminaire Bourbaki 662, (1985) 1-18.
- [15] Daubechies, I., Orthonormal basis of compactly supported wavelets, Commun. Pure Appl. Math. 41, (1988) 909-996.
- [16] Dahmen, W., Kurdila, A., Oswald, P., Multiscale Wavelet Methods for Partial Differential Equations. Academic Press, (1997).
- [17] Bujurke, N.M., Kantli, M. H., Jacobian-free Newton-Krylov subspace method with wavelet-based preconditioner for analysis of transient elastohydrodynamic lubrication problems with surface asperities, Applied Mathematics and Mechanics, 41, (2020) 881-898.
- [18] Bujurke, N.M., Kantli, M. H., Shettar, B.M., Wavelet preconditioned Newton-Krylov method for elastohydrodynamic lubrication of line contact problems, Applied Mathematical Modelling, 46, (2017) 285-298.
- [19] Bujurke, N. M., Salimath, C. S., Kudenatti, R. B., Shiralashetti, S. C., Analysis of modified Reynolds equation using the wavelet-multigrid scheme. Num. Methods Part. Differ. Eqn. 23, (2006) 692-705.
- [20] Shiralashetti, S. C., Kantli, M. H., Deshi, A. B., Mutalik Desai, P. B., A modified wavelet multigrid method for the numerical solution of boundary value problems. J. Inform. Optimiz. Sci. 38:1, (2017) 151-172.
- [21] Kantli, M. H., Shiralashetti, S.C., Finite difference Wavelet-Galerkin method for the numerical solution of elastohydrodynamic lubrication problems, Journal of Analysis, 26:2, (2018) 285-295.
- [22] Shiralashetti S. C., Kantli M. H., Deshi A. B., Wavelet Lifting Scheme for the Numerical Solution of Dynamic Reynolds Equation for Micropolar Fluid Lubrication, Journal of Computational Methods, 18:9, (2021) 2150033.
- [23] Kantli, M. H., Bujurke, N. M., Jacobian free Newton-GMRES method for analysing combined effects of surface roughness and couple stress character of lubricant on EHL line contact, Proceedings of the Indian National Science Academy, 83:1, (2017) 175-196.
- [24] Jensen, A., la Cour-Harbo, A., The Discrete Wavelet Transform: Ripples in Mathematics, Springer, Berlin, (2001).
- [25] Sweldens, W., The lifting scheme: A custom-design construction of biorthogonal wavelets. Appl. Comput. Harmon. Analysis, 3 (2), (1996) 186-200.
- [26] Daubechies, I., Ten lectures on wavelets. CBMS-NSF, SIAM, (1992).
- [27] Soman, K. P., Ramachandran, K. I., Insight in to wavelets, form theory to practice. PHI, Pvt. Ltd. India, (2005).
- [28] Ruch, D. K., Fleet, P. J. V., Wavelet theory an elementary approach with applications. John Wiley and Sons, (2009).
- [29] Pinkus, O., Sternlicht, B., Theory of Hydrodynamic Lubrication, McGraw-Hill, New York, (1961).
- [30] Daubechies, I., Sweldens, W., Factoring wavelet transforms into lifting steps. J. Fourier Anal. Appl. 4 (3), (1998) 247-269.